# Study of Radiative MHD Slip Flow of Williamson Fluid over A Melting Stretching Surface

**Ravi Gupta[a], Manish Gaur[b], Praveen Kumar Dadheech[c]**
[a]School of Science And Technology, Vardhman Mahaveer Open University, Kota, India, 324010
[b]Department of Mathematics, Government PG College, Kota, India 324010
[c]Department of Mathematics, University of Rajasthan, Jaipur, India 302004
(Dadheech (Agrawal (Sharma)

## Abstract

Heat transfer of the boundary layer slip flow in the presence of an inclined magnetic field in a porous medium over a melting stretching surface, is investigated. Also the non-uniform radiation and heat source applied to the flow. Non-linear chemical reaction and entropy generation on Williamson fluid flow studied in this investigation. The equations of the governing flow are transformed into the ordinary differential equations with the help of similarity analysis. Then the reduced system of equations was dealt with Shooting Technique alongside the Runge-Kutta method of order four. Numerical results are presented graphically for velocity and temperature and concentration profiles. From our results after comparing with available literature, results indicates that the entropy generation can be increased with increasing values of parameter of porosity, magnetic field parameter, temperature and concentration slip parameters and decreasing values of slip parameter.

**KEYWORD:** Williamson fluid; Entropy generation; Thermal radiation; Heat source; Inclined MHD; Mass Transfer; Heat Transfer.

**Nomenclature:**

| | |
|---|---|
| $d_1 = L_1\sqrt{\frac{b}{\nu}}$ | Velocity slip parameter |
| $d_2 = L_2\sqrt{\frac{b}{\nu}}$ | Energy slip parameter |
| $d_3 = L_3\sqrt{\frac{b}{\nu}}$ | Mass slip parameter |
| $Br = \frac{\mu b^2 x^2}{k\Delta T}$ | Brinkman number |
| $We = \Gamma x\sqrt{\frac{2b^3}{\nu}}$ | Williamson parameter |
| $K = \frac{\nu}{K_p b}$ | Porosity |

| | |
|---|---|
| $Ec = U^2 / C_p(T_W - T_\infty)$ | Eckert number |
| $L = \frac{RD(C_w - C_\infty)}{k}$ | Diffusion parameter |
| $K_n = \frac{k_n}{b}(C_w - C_\infty)^{n-1}$ | Chemical reaction Parameter |
| $Me = \frac{(T_w - T_\infty)c_p}{(\beta_m + c_s(T_m - T_0))}$ | Melting surface Parameter |
| $M = \frac{\sigma B_0^2}{\rho b}$ | Magnetic field Parameter |
| $R = \frac{4\sigma T_\infty^3}{kk*}$ | Parameter of Radiation |
| $N_S = \frac{\upsilon S_G T_\infty}{bk\Delta T}$ | Entropy generation rate |
| $\Pr = \frac{k}{\mu C_p}$ | Prandtl number |
| $Sc = \frac{\nu}{D_m}$ | Schmidt number |
| $k$ | Thermal conductivity |
| $k*$ | Thermal radiation parameter |
| $c_s$ | Heat capacity |
| Re | Local Reynolds number |
| S | Suction/Injection parameter |
| T | Temperature |
| $T_\infty$ | Ambient fluid temperature |
| $\theta_w = \frac{T_w}{T_\infty}$ | Temperature difference parameter |
| $\alpha_1 = \frac{T_w - T_\infty}{T_\infty}$ | Temperature difference parameter |
| $\alpha_2 = \frac{C_w - C_\infty}{C_\infty}$ | Concentration difference parameter |
| $\beta_m$ | Latent heat |

## 1. Introduction:

Laminar boundary layer flow of non-Newtonian fluid, over a stretching/shrinking surface in a porous medium, however, hasrich implication in the fields of materials science and chemical sciences. Due to their huge engineering applications as, pipe production, plastic films drawing, blood treatment, the analysis of heat transfer of laminar flow and over an expanding surface has gained significant interest.The pivotal work of Blassius was extended by Sakiadis [1], who replaced flat plat with the moving solid surface to investigate boundary layer flow. The study of a wide range of physical parameter involved in Sakiadis work was carried by Erickson et al. [2] on a continuously moving surface which leads to much industrial importance. In this extension Crane [3] analyzed the flow past an extending sheet by assuming that the plate's stretching velocity and its distance from the slit is proportional, such cases mostly occurs in the extrusion of plastics film and polymer industry. Gupta and Gupta [4] added suction and blowing to the boundary surface while Gubka and Bobba [5] considered surface with variable temperature and investigated the boundary layer flow, which was further advanced by Chen and Char [6], who presented a number of closed-form analytical answers for a variety of situations. Bestman [7] studied the mass and heat transfer along a semi-infinite porous channel limited by a vertical permeable surface with a simple model of chemical reaction effects. Keeping in view the fluid flow in manufacturing processes, Ali [8] focused on the general power law of temperature and velocity distribution on surface with several other parameters to model the flow conditions. Rasool et al [9] studied the Williamson nanofluid flow by considering the non-linearly stretching surface and analyze the flow numerically. Study of fluid flow over a stretching surface with various geometries and fluids have been presented by many researchers [10-14]

The study of the flow of the fluid, which is electrically conducted, with imposed magnetic field, is defined as Magnetohydrodynamics (MHD). Applications of MHD can be seen in various technological and engineering fields, for instance geophysics, petroleum industries, MHD flow meters, MHD electricity generators, crystal magnetic infiltration control, advanced magnetic filtration control and MHD pumps etc. MHD can be used as a very important tool for controlling mass and heat transfer. The impact of imposed magnetic field where the sheet is expending exponentially in verity of states was studied by the researchers like Prasanna kumaraet al.[15], Hayat*et al*. [16], Agrawal et al. [17] and Rashad *et al.* [18].

Williamson [19] explored a fluid having shear thinning qualities and both elastic and viscous properties in 1929 and called it the Williamson fluid.Williamson investigated experimentally the pseudo plastic flow materials and developed governing equations to explain the flow of pseudo plastic fluids. The Williamson fluid is one the most essential non-Newtonian fluids having reduced viscosity as shear stress rises and features that are quite comparable to polymeric solutions. In other words, in the Williamson fluid, the functional viscosity should decrease forever as the shear rate rises with infinite viscosity at rest and nil viscosity as the shear rate approaches infinity. Kumar et al. [20] investigated the MHD flow of Williamson fluid over a curved sheet considering non-uniform heat source/sink. Megahed [21] studied thermal radiation and viscous dissipation effect for Williamson fluid flow over a nonlinearly stretching surface.Williamson fluid have been studied by various researchers on various parameters due to its wide applications [22-27]

Entropy generation evidently mentions the energy losses in a system under consideration and applications concerning essentially freezing of modern electronic equipment, geothermal power systems etc. Bejan et al. [28-9] originally formulated Entropy Generation in Convective Heat Transfer also taken into an account Second Law Analysis. Weigand et al. [30] investigated analytically entropy production by Entropy Transport Equation. Makinde et al. [31] scrutinized the entropy optimization for heated plate analytically. Tshehla et al. [32] thrash out rate of entropy optimization in viscous flow through two concentric cylindrical pipes. Liu et al. [33-34] investigated numerically entropy generation in the flow of mixed convection between parallel-plate and isothermal cylinders. Coming after, several researchers [35-39] have excellently applied their tactics for different geometrical configurations to calculating the entropy generation.

A study of entropy optimization on Williamson fluid with mass and heat transfer of MHD slip through permeable medium over a melting expending surface, with an imposed heat source and non-uniform radiation is studied. The impact of physical quantities is explored using graphs. A comparative study with previous findings of researchers is discussed. With the presenting of reliable conclusions, a high level of agreement is attained with the previously published articles.

## 2. Mathematical Modeling:

The velocity, temperature and concentration slip flow of incompressible steady fluid flow with entropy analysis on inclined MHD is studied in 2-D. Porous and melting stretching surface is chosen. Let the surface is extended via velocity $bx$ along the *x-axis* where b is taken as non-negative constant. The fundamental governing equations are as:

$$\frac{\partial u}{\partial x}+\frac{\partial v}{\partial y}=0. \quad (1)$$

$$u\frac{\partial u}{\partial x}+v\frac{\partial u}{\partial y}=-\left(\frac{\sigma B_0^2}{\rho}+\frac{v}{K_p}\right)u+v\frac{\partial^2 u}{\partial y^2}+\sqrt{2}\Gamma\frac{\partial u}{\partial y}\frac{\partial^2 u}{\partial y^2}. \quad (2)$$

$$u\frac{\partial T}{\partial x}+v\frac{\partial T}{\partial y}=\frac{B_0^2\sigma}{C_p\rho}u^2-\frac{1}{C_p\rho}\frac{\partial q_r}{\partial y}+\frac{q'''}{C_p\rho}+\frac{k}{C_p\rho}\frac{\partial^2 T}{\partial y^2}. \quad (3)$$

$$u\frac{\partial C}{\partial x}+v\frac{\partial C}{\partial y}=-k_n(C-C_\infty)^n+D_m\frac{\partial^2 C}{\partial y^2}. \quad (4)$$

Here$u$ and $v$ are velocity components along horizontal and vertical sides respectively and for other physical quantities involved, refer the mentioned nomenclature.

Here $q''' = \left[(T-T_\infty)B^* + (T_w - T_\infty)A^* f'\right]\dfrac{ku_s(x,t)}{\nu x}$ represents the heat source for $q'''$ is nonnegative and heat sink for $q'''$ is negative.

Here two cases $\left(A^* > 0\ ,\ B^* > 0\right)$ , $\left(A^* < 0\ ,\ B^* < 0\right)$ are considered for heat generation and internal heat absorption accordingly.

$$q_r = -\left(\frac{4\sigma}{3k^*}\right)\frac{\partial T^4}{\partial y} = -\left(\frac{16\sigma}{3k^*}\right)T^3\frac{\partial T}{\partial y} \text{(Agrawal et al. [17]).}$$

For above problem boundary condition is given as:

$$u = u_w + L_1\frac{\partial u}{\partial y},\quad v = \frac{k}{\left(\rho(\mathrm{T}_w - \mathrm{T}_0)c_s + \rho\beta_m\right)}\frac{\partial T}{\partial y} - v_w,\quad T = L_2\frac{\partial T}{\partial y} + T_w,\quad C = L_3\frac{\partial C}{\partial y} + C_w \quad \text{at } y = 0,$$

$$u \to 0,\quad T \to T_\infty,\ \text{and}\ C \to C_\infty \quad \text{as} \quad y \to \infty. \tag{5}$$

**3. Solution:**

Proposed similarity transformation for u and v are represented as:

$$u = xbf'(\eta),\qquad v = -(\nu b)^{\frac{1}{2}} f(\eta),\quad \eta = y\sqrt{\frac{b}{\nu}},\ \phi(\eta) = \frac{C_\infty - C}{C_\infty - C_w} \text{ and } \theta(\eta) = \frac{T_\infty - T}{T_\infty - T_w}. \tag{6}$$

Equations (2) and (5) are converted to the following formby applying these transformations:

$$f''' + We\, f''f'''' + f''f - f'^2 - (K_p + M)f' = 0. \tag{7}$$

$$\theta'' + A^* f' + B^*\theta + \frac{4}{3}R\left[3\theta'^2\left((\theta_w - 1)\theta + 1\right)^2 + \left((\theta_w - 1)\theta + 1\right)^3\theta''\right] + \Pr\left(f\theta' + M\,Ecf'^2\right) = 0.$$

(8)

$$\phi'' - \left(K_n\phi^n - f\phi'\right)Sc = 0. \tag{9}$$

The boundary conditions (5) are converted as:

$$f'(\eta) = 1 + d_1 f''(\eta),\ f(\eta) = S + \frac{Me}{\Pr}\theta',\ \theta(\eta) = 1 + d_2\theta'(\eta),\ \phi(\eta) = 1 + d_3\phi'(\eta),\ \text{as}\ \eta = 0,$$

$$f'(\eta) \to 0,\ \theta(\eta) \to 0,\ \phi(\eta) \to 0\ \text{as}\ \eta \to \infty. \tag{10}$$

Now the skin friction coefficient $C_f$ , local Sherwood number $Sh$ and Nusselt number $Nu_x$ are defined as:

$$C_f = \frac{\tau_w}{\rho U_w^2},\ Sh = \frac{J_w x}{(C_\infty - C_w) D_B} \text{ and } Nu_x = \frac{q_w x}{(T_\infty - T_w)} \left.\frac{\partial T}{\partial y}\right|_{y=0}. \qquad (11)$$

Where $\tau_w = \left[ \frac{\Gamma}{2}\left(\frac{\partial u}{\partial y}\right)^2 + \frac{\partial u}{\partial y} \right]\Bigg|_{y=0}$ , $q_w = -\left(k + \frac{16 T_\infty^3 \sigma}{3k^*}\right)\left(\frac{\partial T}{\partial y}\right)\Bigg|_{y=0}$ is surface heat flux and $J_w = -D_B\left(\frac{\partial C}{\partial y}\right)_{y=0}$ is surface mass flux. (12)

Using these values in the equation (11), the following non-dimensional physical parameters are obtained:

$$C_f \operatorname{Re}_x^{\frac{1}{2}} = \left( f'' + \frac{We}{2} f''^2 \right)\Bigg|_{\eta=0}, \qquad (13)$$

$$Nu \operatorname{Re}_x^{\frac{-1}{2}} = -\theta'(0)\left( \frac{4R}{3}\left(1 + (\theta(0)\theta_w - \theta(0))\right)^3 + 1 \right), \qquad (14)$$

$$Sh \operatorname{Re}_x^{-\frac{1}{2}} = -\phi'(0), \qquad (15)$$

**4. Entropy generation model:**

Entropy is a physical phenomenon that is defined as a degree of irreversibility and signifies a disorder in the system and its surroundings. Entropy creation is determined whenever heat is not entirely turned into work. As a result, the following equation is how entropy generation is expressed:

$$S_G = \frac{k}{T_\infty^2}\left(1 + \frac{16\sigma^* T^3}{3kk^*}\right)\left(\frac{\partial T}{\partial y}\right)^2 + \frac{\mu\Gamma}{T_\infty}\left(\frac{\partial T}{\partial y}\right)^3 + \frac{\mu}{T_\infty}\left(\frac{\partial u}{\partial y}\right)^2 + \frac{RD}{T_\infty}\left(\frac{\partial C}{\partial y}\right)\left(\frac{\partial T}{\partial y}\right).$$
$$+ \frac{\sigma}{T_\infty} B_0^2 u^2 + \frac{RD}{C_\infty}\left(\frac{\partial C}{\partial y}\right)^2. \qquad (16)$$

Using Equation(6), this equation is simplified to the following equation:

$$N_G = \left( \alpha_1 + \frac{4\alpha_1 R}{3}\left(1 + (\theta\theta_w - \theta)\right)^3 \right)\theta'^2 + Br.f''^2 + WeBrf''^3$$

$$+Brf'^2(M+Kp)+\frac{\alpha_2}{\alpha_1}L\phi'^2+\theta' L\phi'. \quad (17)$$

The non-dimensional parameters are obtained as follows:

$\alpha_1=-\frac{T_\infty-T_w}{T_\infty}$ Parameter of temperature difference

$\alpha_2=-\frac{C_\infty-C_w}{C_\infty}$ Parameter of concentration difference

$Br=\frac{\mu b^2x^2}{k\Delta T}$ Brinkman number

$L=\frac{\mathrm{RD}(C_w-C_\infty)}{k}$ Diffusion parameter

$N_S=\frac{vS_GT_\infty}{bk\Delta T}$ Entropy generation rate

**5. Result and Discussions:**

A study of second law analysis for Williamson fluid flow for heat transfer and chemical reaction is studied. In a porous medium over a melting stretching surface with slip condition and nonlinear thermal radiation is considered in this investigation. Also the effect of inclined magnetic field with heat source is discussed here. Using above numerical method, results are obtained for several physical dimensionless parameters which are represented by the graphs. The results are obtained to illustrate influence of various physical parameters for temperature profile $\theta(\eta)$, velocity profile $f'(\eta)$ and temperature gradient profile $\phi(\eta)$. The non-dimensional parameters are studied in the following ranges: $0\le M\le 2,\ 0\le K_p\le 1,\ 0\le Me\le 1,$ $0\le d_1\le 0.2,\ 0\le d_2\le 1,\ 0\le d_3\le 1,$ $1\le n\le 3,$ $0\le S\le 1, 0\le Ec\le 2,\ 1\le Sc\le 3,$ $1\le\theta_w\le 2,\ 0.5\le\beta\le\infty,$ $0\le Kn\le 1, 0\le A^*\le 2, 0\le B^*\le 2.$, While graphical depiction of any parameter the other fixed values of the parameters are considered as $\beta=2.0,\ \ \delta_1=\delta_2=\delta_3=0.1,\ \theta_w=0.2,\ \ A^*=0.2,\ \ B^*=0.1$ $Kn=0.2,\ Ec=0.2,$ and $Kn=0.2$ .A comparison of results is also mentioned, along with well-known results (Table 4-5). Our outputs are a perfect match for all these outcomes.

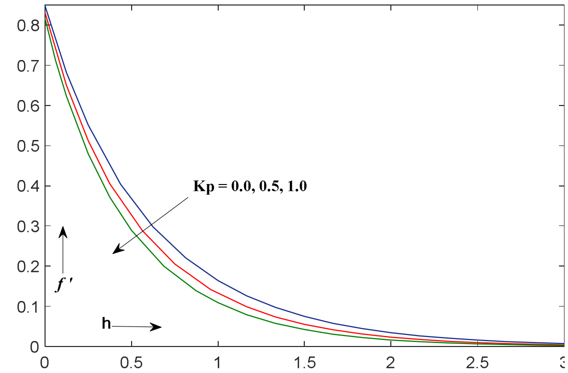


Figure1. Effect of parameter of Kp onvelocity profile

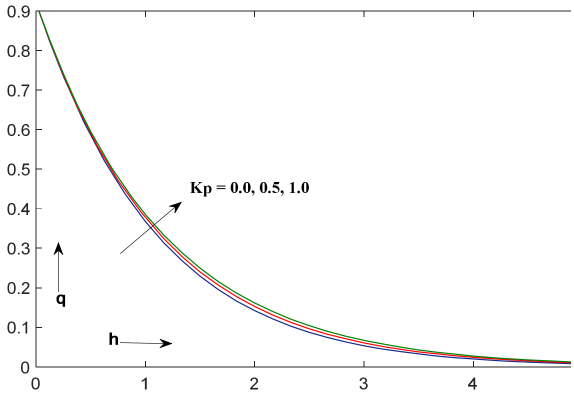


Figure 2. Effect of parameter Kp ontemperature profile

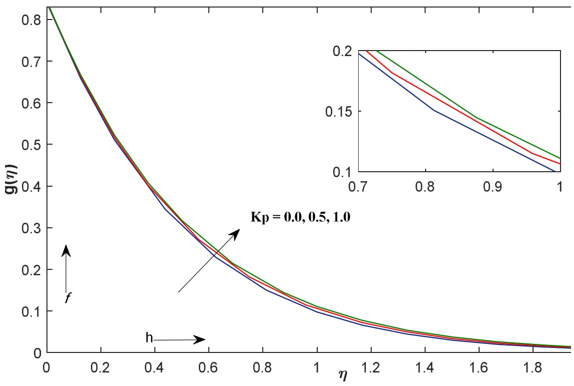


Figure 3. Effect of parameter Kp onmass profile

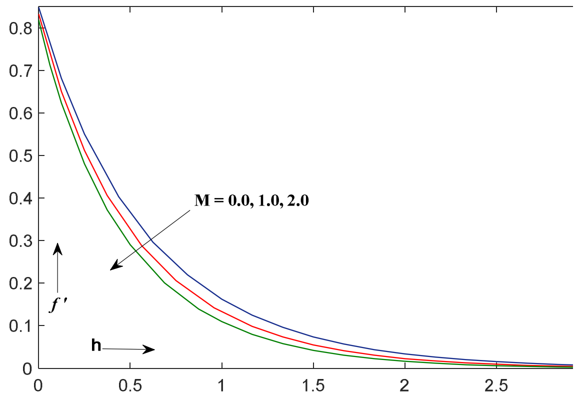


Figure 4. Effect of parameterM onvelocity profile

The effects of permeability parameter $K_p$ are depicted for velocity, temperature and concentration profiles by Figure 1, Figure 2 and Figure 3 accordingly. With an increment in the values of parameter $K_p$, continuous decrement is noted for velocity profile. Also reverse effects are noticed for temperature and mass profile with increased *M*. As porosity increases, the porous medium's permeability decreasesbecause $K_p \propto \frac{1}{K}$.

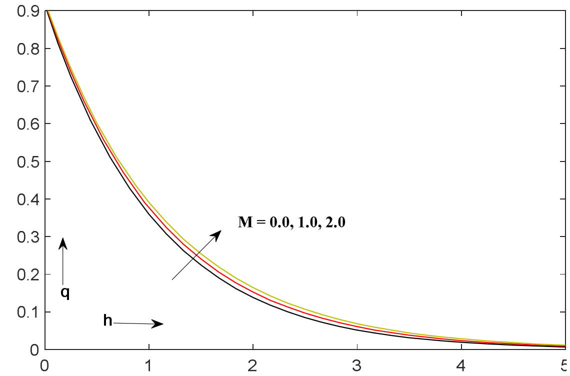


Figure 5. Effect of parameter Mon temperature profile

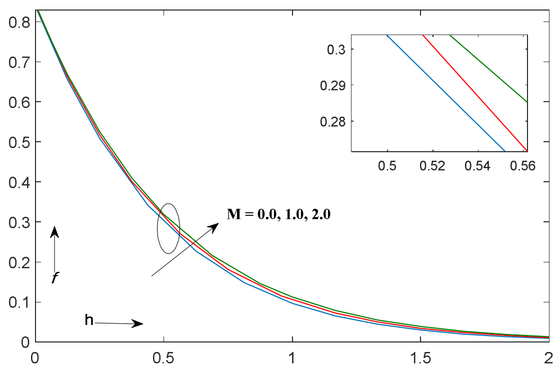


Figure 6. Effect of parameter M on concentration profile

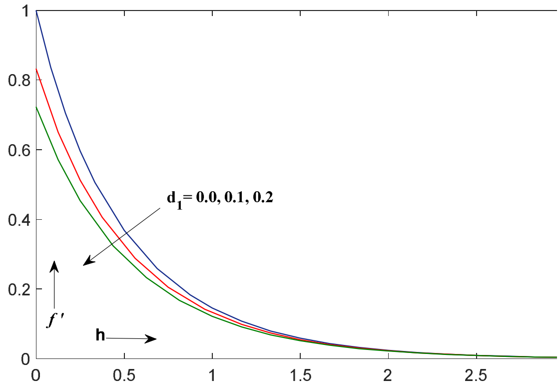


Figure 7. Effect of parameter $d_1$ on velocity profile

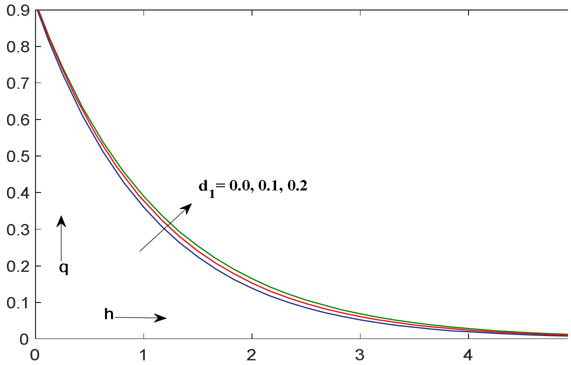


Figure 8. Effect of parameter $d_1$ on temperature profile

The magnetic field effects on the flow are depicted for velocity, temperature and concentration profiles by Figure 4, Figure 5 and Figure 6 accordingly. Results indicate that with an increment in the values of magnetic field parameter $M$ continuous decrement is noted for velocity profile. Also reverse effects are noticed for temperature and mass profile with increased $M$. More energy produces as the magnetic field is strengthened this result to increased temperature profile. Also due to Lorentz force which resist the flow leads to decreased velocity field.

The velocity slip parameter $d_1$ shows significant effect on velocity and temperature profiles which represented by Figure 7 and Figure 8.The slipping fluid exhibits contraction in skin resistance of the surface existent between the fluid and the surface because the surface dragging force cannot be imparted to the fluid. With increased $d_1$, velocity profile decreases but an increment is seen in temperature profile.

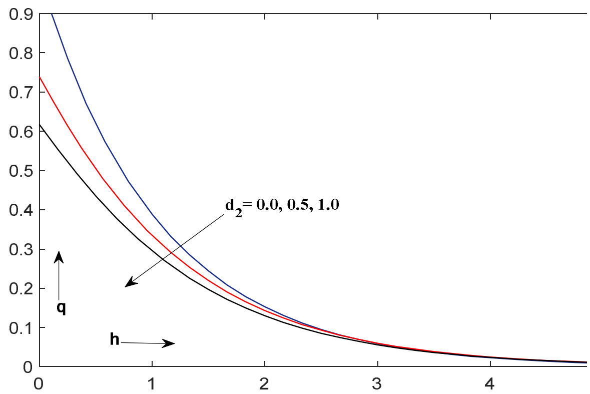


Figure 9. Effect of parameter $d_2$ontemperature profile

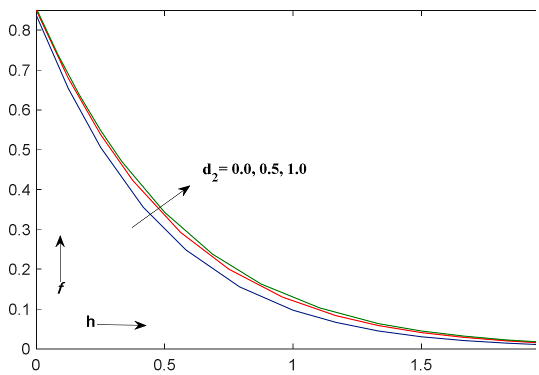


Figure 10. Effect of parameter Impact of $d_2$on mass profile

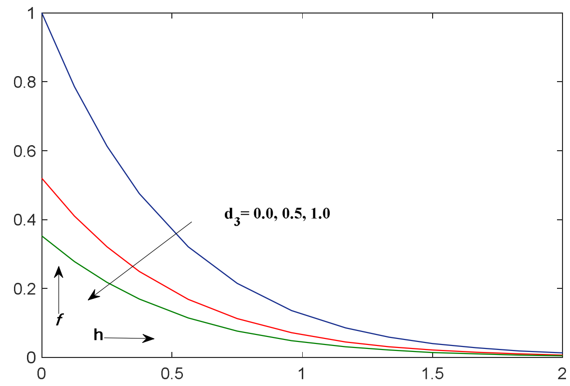


Figure 11. Effect of parameter Impact of $d_3$ on concentration profile

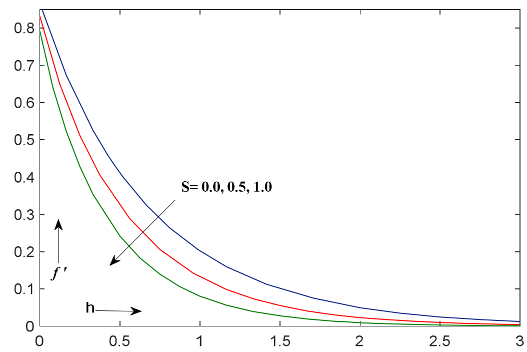


Figure 12. Effect of parameter S onvelocity profile

Similarly Figure 9 and Figure 10depict the impact of temperature slip parameter $d_2$ on velocity and temperature profiles respectively. Results indicate that with enhancing temperature slip parameter velocity profile decreases whereas increment is noticed in temperature profile. Because the rate of heat transport from the sheet to the fluid, decreases when the thermal slip parameter increases. Also the effect of concentration slip parameter $d_3$ is depicted in Figure 11 for concentration profile. By improving the $d_3$ parameter the concentration profile decreases.

The effect of suction parameter *S*, on velocity and temperature profiles which are represented by Figure 12, Figure 13 and Figure 14. All the three profiles show decrement with increasing the parameter S. When $S > 0$, some fluid particles are absorbed by the porous wall, causing the flow velocity to rise, resulting in a smaller thermal boundary layer.As a result, the overall heat and mass exchange efficiency rises as a result of this process.

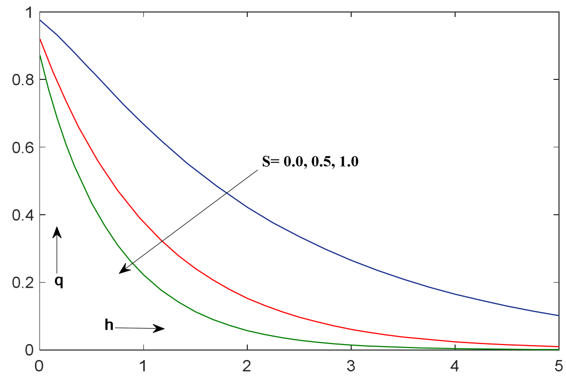


Figure 13. Effect of parameter S on temperature profile

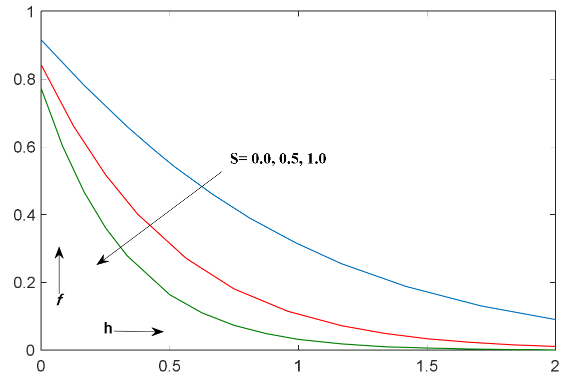


Figure 14. Effect of parameter Impact of S on concentration profile

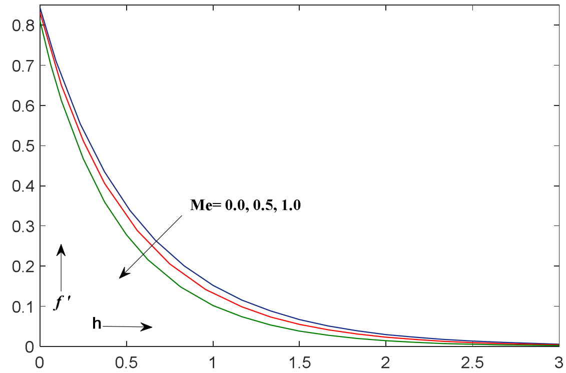


Figure 15. Effect of parameter Me on velocity profile

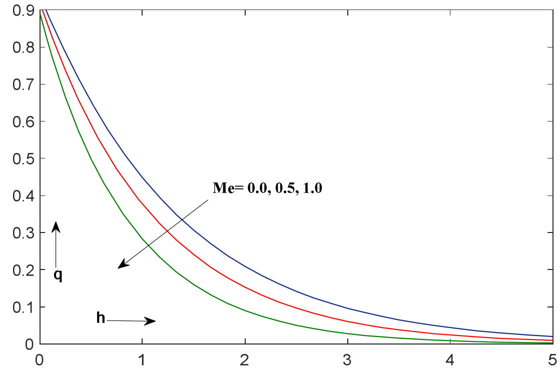


Figure 16. Effect of parameter Me on temperature profile

The effects of melting surface parameter $Me$, on velocity and temperature profiles which are represented by Figure 15, Figure 16 and Figure 17. All the three profiles show decrement with increasing the parameter $Me$.The transport of heat from fluids to surface occurs when the Nussult number becomes negative.Hence a higher melting results in a larger thermal boundary layer and less heat transfer.

The effect of temperature ratio parameter $\theta_w$, on temperature profile is represented by Figure 18.Results shows that the temperature profile increases with increasing $\theta_w$.The effect of $n$, Schmidt number $Sc$ andChemical reaction parameter $Kn$ parameter on concentration profile is depicted by Figures19-21. By improving the parameter $n$,$Sc$ and $Kn$ parameter, the concentration profile gets cut down for $Sc$ and $Kn$ whereas rises for $n$. Because of the characterization of Sc, the mass diffusion coefficient drops as Sc increases, resulting in a lower concentration boundary layer.

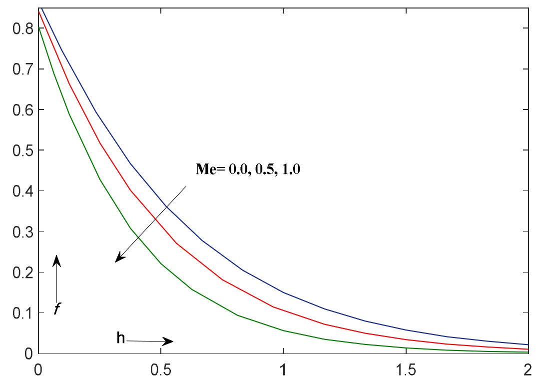


Figure 17. Effect of parameter Me on concentration profile

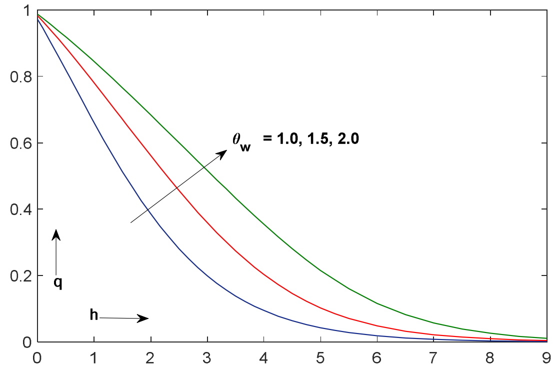


Figure 18. Effect of parameter $\theta_w$ on temperature profile

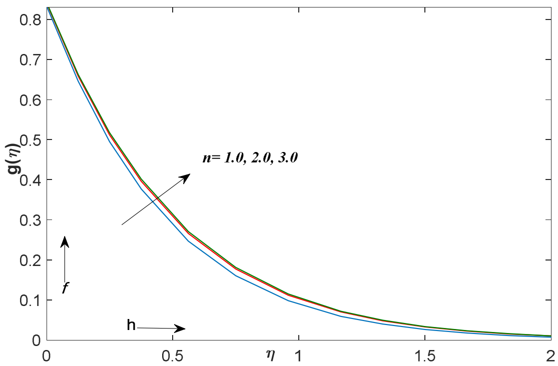


Figure 19. Effect of parameter *n* on concentration profile.

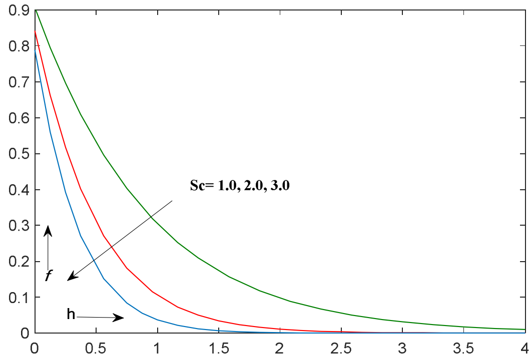


Figure 20. Effect of parameter Sc on concentration profile.

The effect of entropy generation is studied for physical parameters in this investigation and depicted by entropy generation profile. The effects of magnetic field parameter *M*, permeability parameter $K_p$ , suction parameter *S* and melting surface parameter *Me*are depicted by Figure 21,Figure 22, Figure 23 and Figure 24 respectively.The entropy generation enhances by increasing all above parameters. A reverse effect is observed for the velocity slip parameter $d_1$, as depicted by figure 30. Similarly figures (31-33) depicts the impacts of parameters $d_2, d_3$ and *Br* on entropy generation$Ns$. Withincreasing values of the parameter $Br$ entropy generation increases whereas it decreases for $d_2, d_3$ when the values of these parameter get increased.Figures (34-37) represents the impact of parameters$Sc$,$L$,$\alpha_1$,$\alpha_2$ on entropy generation number $Ns$. With increasing the values ofparameters $Sc$, $L$, $\alpha_1$, and $\alpha_2$ parameters, the improved entropy generation is obtained.

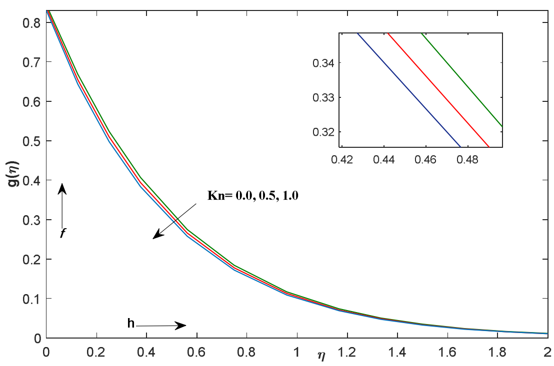


Figure 21. Effect of parameter Kn on concentration profile.

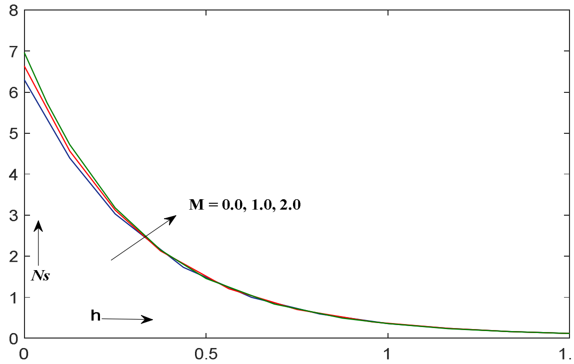


Figure 22. Effect of parameter M on Entropy generation *Ns*.

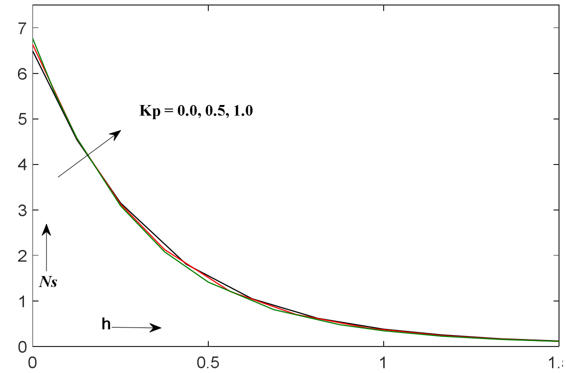


Figure 23. Effect of parameter $K_p$ on Entropy generation *Ns*.

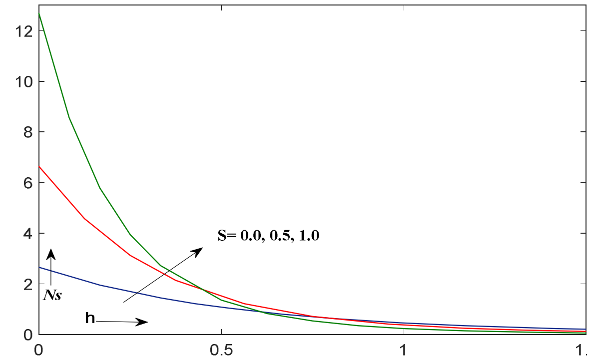


Figure 24. Effect of parameter S on Entropy generation *Ns*.

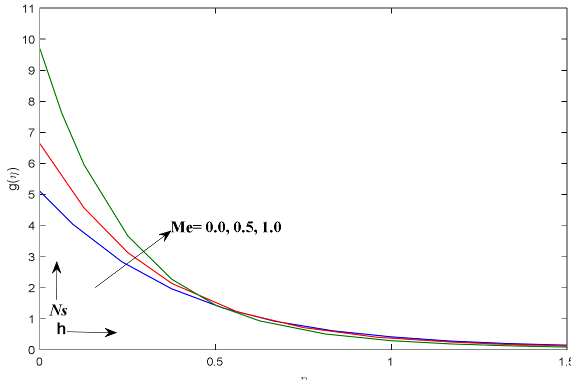


Figure 25. Effect of parameter *Me* on Entropy generation *Ns*.

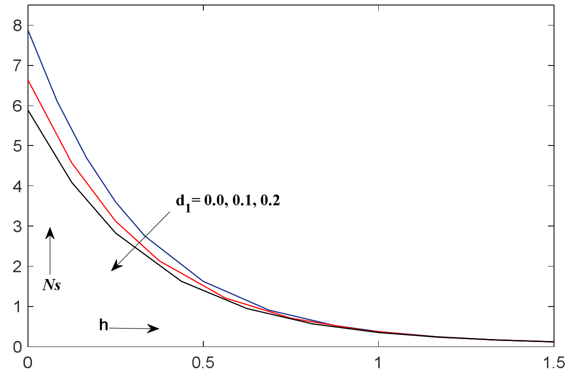


Figure 26. Effect of parameter $d_1$ on Entropy generation *Ns*.

The effects of physical parameters on the skin friction coefficient $c_f \mathrm{Re}_x^{\frac{1}{2}}$, local Sherwood number $Sh\,\mathrm{Re}^{\frac{-1}{2}}$ and local Nusselt number $Nu\,\mathrm{Re}_x^{\frac{-1}{2}}$ is represented by Table 1. From the table it is noticed that with increasing parameter $M$ and parameter $Kp$the skin friction coefficient $c_f \mathrm{Re}_x^{\frac{1}{2}}$ raises whereas a decrement is seen for the local Sherwood number $Sh\,\mathrm{Re}^{\frac{-1}{2}}$ and local Nusselt number $Nu\,\mathrm{Re}_x^{\frac{-1}{2}}$. Also with increasing $Me$parameter an increment is noticed for skin friction coefficient, local Nusselt number and local Sherwood number.

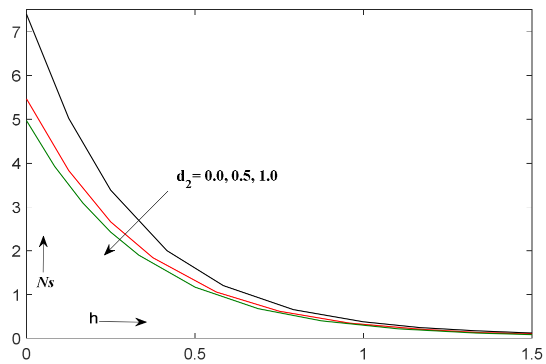


Figure 27. Effect of parameter $d_2$ on Entropy generation *Ns*.

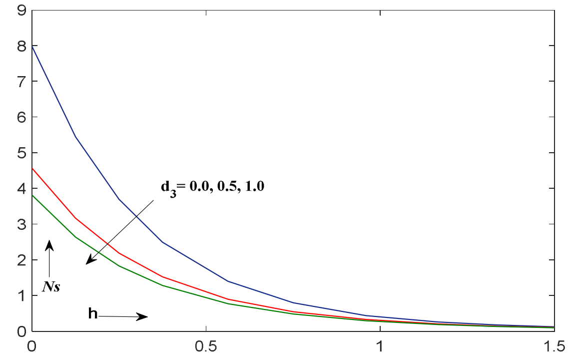


Figure 28. Effect of parameter $d_3$ on Entropy generation *Ns*.

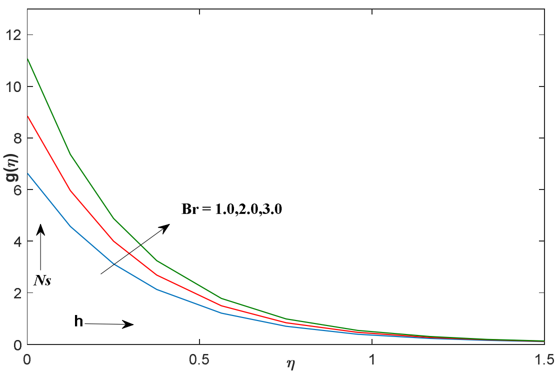


Figure 29. Effect of parameter*Br* on Entropy generation *Ns*.

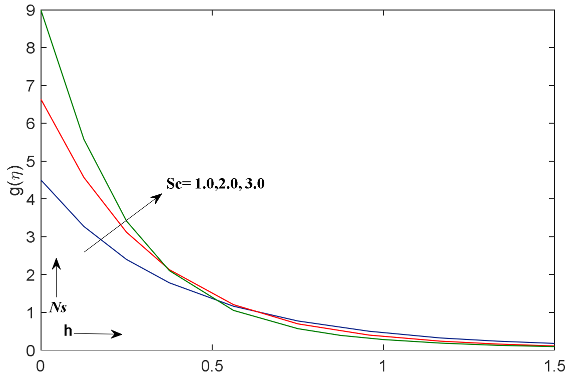


Figure 30. Effect of parameter*Sc* on Entropy generation *Ns*.

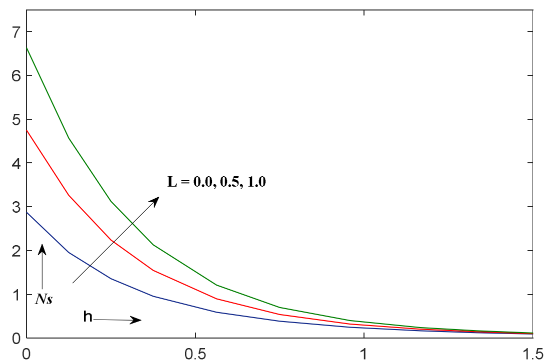


Figure 30. Effect of parameter *L* on Entropy generation *Ns*.

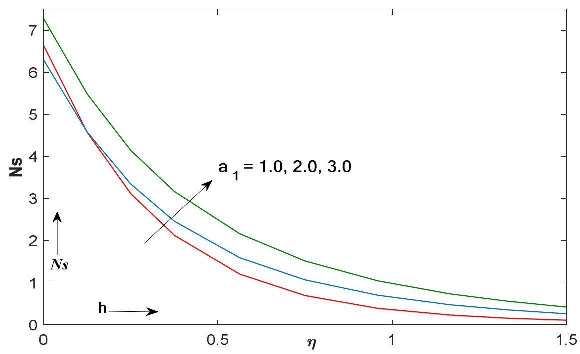


Figure 31. Effect of parameter $\alpha_1$ on Entropy generation *Ns*.

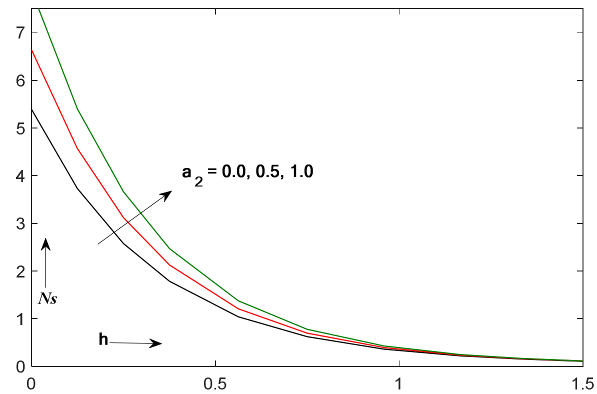


Figure 32. Effect of parameter $\alpha_2$ on Entropy generation *Ns*.

Tables 2 and Table 3 compare the results of the evaluation to those published in earlier research publications, such as Golra and Sidawi [40], Nadeem et al [41], Khan and Pop[42], Prasad et al. [43], Anderson et al. [44], Palani et al.[45]and.In Table 3 comparisons of $-\theta'(0)$ for various values Pr is given considering Me=0; S=0.0; R=0; Kn=0.0; Kp=0; Sc=0.0; $\alpha=\pi/2$; We=0; A*=0.0; Ec=0.0; M=0; B*=0.0; $\varepsilon=0.0$; n=1; $\delta_1=\delta_2=\delta_3=0$. In Table 4 comparisons of $-f''(0)$ for various values of M is given, taking Kp=0, R=0, Me=0, $\alpha=\pi/2$, $\delta_1=\delta_2=\delta_3=0$, We=0, S=0, A*=0.0, $\varepsilon=0.0$, B*=0.0, n=1, Ec=0.0, Sc=0.0, Kn=0.0. As compared the results to those previously published, and it is noticed that they are very similar.

## 6. Conclusion:

Second law analysis for Williamson fluid MHD flow for heat transfer and chemical reaction is studied. In a porous medium over a melting stretching surface with slip condition and nonlinear thermal radiation is considered in this investigation. The significant findings of current study are pointed as:

- The temperature and concentration profiles increases and velocity profile gets cut down for increasing of magnetic field parameter.
- Porosity parameter has propensity to increases the temperature and concentration profiles.
- Entropy generation *Ns* increases for the increasing values of $M$, and $Kp$.
- Entropy generation *Ns* decreases for the decreasing values of $d_1$,$d_2$ and $d_3$ parameters.
- Entropy generation *Ns* increasesfor the increasing values of $Me, Br, \alpha_1$and$\alpha_2$ parameters.

**Table-1**

| For Williamson fluid | | | | | | | | | | | | |
|---|---|---|---|---|---|---|---|---|---|---|---|---|
| M | Kp | $d_1$ | S | Me | $d_2$ | $d_3$ | $q_w$ | A* | n | $-C_f \mathrm{Re}_x^{\frac{1}{2}}$ | - $Nu\,\mathrm{Re}_x^{\frac{-1}{2}}$ | - $Sh\,\mathrm{Re}^{\frac{-1}{2}}$ |
| 0 | | | | | | | | | | 1.285714182 | 0.869075142 | 1.611732916 |

| | | | | | | | | | | | | |
|---|---|---|---|---|---|---|---|---|---|---|---|---|
| 1 | | | | | | | | | | 1.396225868 | 0.820616237 | 1.579424350 |
| 2 | | | | | | | | | | 1.489078645 | 0.780418779 | 1.552046914 |
| | 0 | | | | | | | | | 1.281851798 | 0.831268529 | 1.601312447 |
| | 0.5 | | | | | | | | | 1.396225868 | 0.820616237 | 1.579424350 |
| | 1 | | | | | | | | | 1.491809453 | 0.811186284 | 1.560852579 |
| | | | | | | | | | | 1.285714182 | 0.869075142 | 1.611732916 |
| | | | | | | | | | | 1.396225868 | 0.820616237 | 1.579424350 |
| | | | | | | | | | | 1.489078645 | 0.780418779 | 1.552046914 |
| | | 0 | | | | | | | | 1.713510693 | 0.840575685 | 1.626989311 |
| | | 0.1 | | | | | | | | 1.396225868 | 0.820616237 | 1.579424350 |
| | | 0.2 | | | | | | | | 1.192997850 | 0.804780213 | 1.545020406 |
| | | | 0 | | | | | | | 1.156043641 | 0.244720607 | 0.842601676 |
| | | | 0.5 | | | | | | | 1.396225868 | 0.820616237 | 1.579424350 |
| | | | 1 | | | | | | | 1.646586144 | 1.334479961 | 2.283005811 |
| | | | | 0 | | | | | | 1.318177557 | 0.645201544 | 1.343783398 |
| | | | | 0.5 | | | | | | 1.396225868 | 0.820616237 | 1.579424350 |
| | | | | 1 | | | | | | 1.530291775 | 1.103206139 | 1.966095693 |
| | | | | | 0 | | | | | 1.412127175 | 0.971958698 | 1.626515510 |
| | | | | | 1 | | | | | 1.368737194 | 0.568644349 | 1.497247385 |
| | | | | | 2 | | | | | 1.355154937 | 0.448230708 | 1.456332738 |
| | | | | | | 0 | | | | 1.396225868 | 0.820616237 | 1.894108172 |
| | | | | | | 1 | | | | 1.396225868 | 0.820616237 | 0.960360815 |
| | | | | | | 2 | | | | 1.396225868 | 0.820616239 | 0.647639828 |
| | | | | | | | 1 | | | 1.345054448 | 0.649446952 | 1.425726308 |
| | | | | | | | 1.5 | | | 1.334997319 | 0.946160880 | 1.395147703 |
| | | | | | | | 2 | | | 1.330422126 | 1.457715771 | 1.381203778 |
| | | | | | | | | 0 | | 1.402703647 | 0.889117650 | 1.598657188 |
| | | | | | | | | 1 | | 1.366369317 | 0.506351438 | 1.490169861 |
| | | | | | | | | 2 | | 1.317221781 | 0.010085049 | 1.340848436 |
| | | | | | | | | | 1 | 1.396225868 | 0.820616237 | 1.663080172 |
| | | | | | | | | | 2 | 1.396225868 | 0.820616237 | 1.602010098 |
| | | | | | | | | | 3 | 1.396225868 | 0.820616237 | 1.579424350 |
| Local Sherwood number $Sh$ for following physically parameter. | | | | | | | | | | | | |
| Sc | Kn | | | | | | | | | | | |
| 1 | | | | | | | | | | 1.396225943 | 0.820616388 | 0.936046713 |
| 2 | | | | | | | | | | 1.396225868 | 0.820616237 | 1.579424350 |
| 3 | | | | | | | | | | 1.396225450 | 0.820616237 | 2.106246818 |
| | 0.0 | | | | | | | | | 1.396225868 | 0.820616237 | 1.546844472 |
| | 0.5 | | | | | | | | | 1.396225868 | 0.820616237 | 1.625467421 |
| | 1.0 | | | | | | | | | 1.396225868 | 0.820616237 | 1.695826645 |

**Table-2**

| Pr | Comparing with previous studies of of $-\theta'(0)$ for various values Pr considering Me=0; S=0.0; R=0; Kn=0.0; Kp=0; Sc=0.0; $\alpha = \pi/2$; We=0; A*=0.0; Ec=0.0; M=0; B*=0.0; $\varepsilon$ =0.0; n=1; $\delta_1 = \delta_2 = \delta_3$ =0. | | | |
|---|---|---|---|---|
| | Golra and Sidawi [40] | Nadeem et al. [41] | Khan and Pop [42] | Present study |
| 0.7 | 0.454 | 0.454 | 0.454 | 0.454049247 |
| 2.0 | 0.911 | 0.911 | 0.911 | 0.911360654 |

**Table-3**

| Comparing with previous studies of $-f''(0)$ for various values of M taking Kp=0, R=0, Me=0, $\alpha = \pi/2$, $\delta_1 = \delta_2 = \delta_3$ =0, We=0, S=0, A*=0.0, $\varepsilon$ =0.0, B*=0.0, n=1, Ec=0.0,Sc=0.0, Kn=0.0. | | | | |
|---|---|---|---|---|
| M | Prasad et al. [43] | Anderson et al. [44] | Palani et al [45] | Present study |
| 0 | 1.000174 | 1.0000 | 1.000000 | 1.000001172 |
| .5 | 1.224753 | 1.2249 | 1.224745 | 1.224744872 |
| 1 | 1.414449 | 1.4140 | 1.414214 | 1.414213563 |
| 1.5 | 1.581139 | 1.5810 | 1.581139 | 1.581138831 |
| 2 | 1.732203 | 1.7320 | 1.732051 | 1.732050807 |

**References:**


1. Sakiadis,B.C., Boundary-layer behavior on continuous solid surface: II. The boundary layer on a continuous flat surface, *American Institute of Chemical Engineering Journals*, 7 (2) (1961) 221-225.
2. Erickson,L.E., Fan,L.T. and Fox,V.G., Heat and mass transfer on a moving continuous flat plate with suction or injection, *Industrial & Engineering Chemistry Fundamentals*, 5 (1) (1966) 19-25.
3. Crane,L.J., Flow past a stretching plate, *Journal of Applied Mathematics and Physics (ZAMP)*, 21 (4) (1970) 645–647.
4. Gupta,P.S. and Gupta,A.S., Heat and mass transfer on a stretching sheet with suction and blowing, *The Canadian Journal of Chemical Engineering*, 55 (1977) 744-756.
5. Grubka,L.G. andBobba,K.M., Heat transfer characteristics of a continuous stretching surface with variable temperature, *The ASME Journal of Heat Transfer*, 107 (1985) 248–250.

6. Chen,C.K. and Char,M.I., Heat transfer of a continuous stretching surface with suction or blowing, *Journal of Mathematical Analysis and Applications*, 135 (2) (1988) 568–580.
7. Bestman,A.R., Natural convection boundary layer with suction and mass transfer in a porous medium, *International Journal of Energy Research*, 14 (1990) 389-396.
8. Ali,M.E., On thermal boundary layer on a power law stretched surface with suction or injection, *International Journal of Heat and Fluid Flow*, 16 (4) (1995) 280-290.
9. Rasool, G., Zhang, T. Chamkha, A.J.,Shafiq, A.,Tlili, I. andShahzadi, G., Entropy generation and consequences of binary chemical reaction on MHD Darcy–Forchheimer Williamson nanofluid flow over non-linearly stretching surface. *Entropy*, 22, (2020), 18.
10. P. Agrawal, P.K. Dadheech, R.N. Jat, M. Bohra, K.S. Nisar, I. Khan, Lie similarity analysis of MHD flow past a stretching surface embedded in porous medium along with imposed heat source/sink and variable viscosity, Journal of Materials Research and Technology,9(5) (2020), 10045-10053.
11. R.N. Jat, P Agrawal, PK Dadheech. MHD boundary layer flow and heat transfer of Caisson fluid over a moving porous plate with viscous dissipation and thermal radiation effects, Journal of Rajasthan Academy of Physical Sciences 16 (3-4) (2017), 211-232.
12. Dadheech, P.K., Agrawal, P., Mebarek-Oudina, F., Abu-Hamdeh, N. and Sharma, A., 2020, Comparative Heat Transfer Analysis of MoS 2 /C 2 H 6 O 2 and SiO 2 -MoS 2 /C 2 H 6 O 2 Nanofluids with Natural Convection and Inclined Magnetic Field. Journal of Nanofluids, 9(3), pp. 161-167.
13. Agrawal, P., Dadheech, P.K., Jat, R.N., Nisar, K.S., Bohra, M. and Purohit. S.D., 2021, Magneto Marangoni flow of γ−AL2O3 nanofluids with thermal radiation and heat source/sink effects over a stretching surface embedded in porous medium. *Case Studies in Thermal Engineering*, 23, pp. 100802. https://doi.org/10.1016/j.csite.2020.100802.
14. Dadheech, P.K., Agrawal, P., Sharma, A., Nisar, K.S. and Purohit, S.D., 2021, Marangoni convection flow of γ–Al2O3 nanofluids past a porous stretching surface with thermal radiation effect in the presence of an inclined magnetic field. *Heat Transfer*. pp. 1- 17. https://doi.org/10.1002/htj.22318.
15. Prasannakumara,C.,Gireesha,B.J.,Gorla,R.S.R. and Krishnamurthy,M.R.,Effects of chemical reaction and nonlinear thermal radiation on Williamson nanofluid slip flow over a stretching sheet embedded in a porous medium, *Journal of Aerospace Engineering*, 29(5), (2016), 04016019
16. Hayat,T.,Bibi,S.,Rafiq,M.,Alsaedi,A. andAbbasi,F.M., Effect of an inclined magnetic field on peristaltic flow of Williamson fluid in an inclined channel with convective conditions, *J. Magn. Magn. Mater.*, 401, (2016), 733–745.
17. Agrawal, P., Dadheech, P.K., Jat, R.N., Baleanu, D. and Purohit, S.D., 2021, Radiative MHD hybrid-nanofluids flow over a permeable stretching surface with heat source/sink embedded in porous medium, *International Journal of Numerical Methods for Heat & Fluid Flow*, 31(8),(2021), 2818-2840.

18. Rashad,A.M.,Rashidi,M.M.,GiulioLorenzini, Sameh E. Ahmed, Abdelraheem M. Aly, Magnetic field and internal heat generation effects on the free convection in a rectangular cavity filled with a porous medium saturated with Cu–water nanofluid, Int. J. Heat Mass Transf. 104 (2017) 878–889.
19. Williamson,R.V., The flow of pseudoplastic materials, Industrial & Engineering Chemistry, 21(11), (1929), 1108–1111.
20. Kumar, K.A.; Reddy, J.V.R.; Sugunamma, V.; Sandeep, N. Simultaneous solutions for MHD flow of Williamson fluid over a curved sheet with nonuniform heat source/sink. Heat Transf. Res. 50,( 2019), 581–603.
21. Megahed, A.M. (2019). Williamson fluid flow due to a nonlinearly stretching sheet with viscous dissipation and thermal radiation. Journal of the Egyptian Mathematical Society, 27: 12. http://doi.org/10.1186/s42787-019- 0016-y
22. Nagendra, N., Amanulla., C.H., Reddy, M.S., Slip effects on MHD flow of a Williamson fluid from an isothermal sphere: A numerical study. *AMSE JOURNALS-AMSE IIETA publication-2017-Series: Modelling B*, 86(3), (2017), 782-807.
23. Panezai, A.,Rehman, A., Sheikh, N.,Iqbal, S., Ahmed, I.,Iqbal, M. andZulfiqar, M., Mixed convective magnetohydrodynamic heat transfer flow of Williamson fluid over a porous wedge. *Am. J. Math. Comput. Model*, 4, (2019), 66–73.
24. Ahmed, K.; Akbar, T. Numerical investigation of magnetohydrodynamics Williamson nanofluid flow over an exponentially stretching surface. *Adv. Mech. Eng.*, 13, (2021), 168781402110198.
25. Dadheech, P.K., Agrawal, P., Sharma, Dadheech, A., Mdallal, Q.A. and Purohit, S.D., Entropy analysis for radiative inclined MHD slip flow with heat source in porous medium for two different fluids, Case Studies in Thermal Engineering, 28, (2021), 101491.
26. Ibrahimt,W. and Negera,M., The Investigation of MHD Williamson Nanofluid over Stretching Cylinder with the Effect of Activation Energy, *Advances in Mathematical Physics*, 2020, (2020), 1-16.
27. Endalew,M.F. andNayak,A., Thermal radiation and inclined magnetic field effects on MHD flow past a linearly accelerated inclined plate in a porous medium with variable temperature, *Heat Transf. Asian Res*., 48, (2019), 42–61.
28. Magyari,E.and Pantokratoras,A., Note on the effect of thermal radiation in the linearized Rosseland approximation on the heat transfer characteristics of various boundary layer flows.*International Communication Heat Mass Transf*er, 38, (2011), 554-556.
29. Ganesh Kumar,K.,Rudraswamy,N.G.,Gireesha,B.J. andManjunatha,S.Non linear thermal radiation effect on Williamson fluid with particle-liquid suspension past a stretching surface, *Results in Physics*, 7, (2017), 3196-3202
30. Sacheti,N.C., Bashir,T.E., and Chandran,P., Perturbation analysis of 2-dimensional boundary layer flow of an inelastic fluid using Williamson model, *International Journal of Applied Engineering Research*, 22, (2017), 12728–12734.
31. Bejan, A., A study of Entropy Generation in Fundamental Convective Heat ransfer. *J. Heat Trans-T ASME*,101, (1979), 718–725.

32. Bejan, A., Second Law Analysis in Heat Transfer and Thermal Design. *Adv. Heat Transfer*,15, (1982), 1–58.
33. Weigand, B.,Birkefeld, A., Similarity Solutions of the Entropy Transport Equation. *Int. J. Therm. Sci.*, 48, (2009), 1863–1869.
34. Makinde, O.D., Thermodynamic second law analysis for a gravity-driven variable viscosity liquid film along an inclined heated plate with convective cooling. *J. Mech. Sci. Technol*., 24, (2010), 899–908.
35. Tshehla, M.S.,Makinde, O.D., Analysis of Entropy Generation in a Variable Viscosity Fluid Flow Between Two Concentric Pipes with Convective Cooling at the Surface. Int. J. Phys. Sci., 6 (2011), 6053–6060.
36. Liu, C.C., Chen, C.K. Lai, H.Y., Numerical Analysis of Entropy Generation in Mixed Convection Flow with Viscous Dissipation Effects in Vertical Channel. *Int. Commun. Heat Mass*, 38, (2011), 285–290.
37. Liu, C.C., Lo, C.Y., Numerical Analysis of Entropy Generation in Mixed-Convection MHD Flow in Vertical Channel. *Int. Commun. Heat Mass*, 39, (2012), 1354–1359.
38. Ganesh, N.V., Al-Mdallal, Q.M. and Chamkha, A.J., A numerical investigation of Newtonian fluid flow with buoyancy, thermal slip of order two and entropy generation, *Case Studies in Thermal Engineering*, 13, (2019), 100376.
39. Qayyum, S.Sumaira, Khan, M.,Masood, F., Chu, Y.M.,Kadry, S. and Mubbashar, M., Interpretation of entropy generation in Williamson fluid flow with nonlinear thermal radiation and first-order velocity slip. *Mathematical Methods in the Applied Sciences*. 44, (2021), 7756-7765.
40. Reddy, G.J.Kethireddy, B. Kumar, M. andHoque, M.M., A molecular Dynamics Study on Transient Non-Newtonian MHD Casson Fluid Flow Dispersion over a Radiative Vertical Cylinder with Entropy Heat Generation. J. Mol. Liq., 252, (2018), 245–262.
41. Gorla,R.S.R. and Sidawi,I., Free convection on a vertical stretching surface with suction and blowing. *Applied Scientific Research*, 52, (1994), 247-257.
42. Nadeem,S. and Hussain,S.T., Flow and heat transfer analysis of Williamson nanofluid.*Applied Nanoscience*, 19, (2013), 286.
43. Khan,W.A. and Pop,I., Boundary-layer flow of a Nanofluid past a stretching sheet, *International Journal of Heat Mass Transfer*, 53, (2010), 2477-2483.
44. Prasad,K.V.,Sujatha,A.,Vajravelu,K. and Pop,I. MHD flow and heat transfer of a UCM fluid over a stretching surface with variable thermos-physical properties. *Meccanica*, 47, (2012), 1425–39.
45. Andersson,H.I., Hansen,O.R. and Holmedal,B., Diffusion of a chemically reactive species from a stretching sheet. *International Journal of Heat Mass Transfer*, 37, (1994), 659–64.
46. Palani,S., Kumar,B.R. and Kameswaran,P.K. Unsteady MHD flow of an UCM fluid over a stretching surface with higher order chemical reaction, *Ain Shams Engineering Journal*, 7, (2016), 399–408.